Numerical Simulation of a TLP in Large Waves by OpenFOAM

李, 岩松
九州大学大学院総合理工学府総合理工学専攻機械・システム理工学メジャー

https://hdl.handle.net/2324/6788227

出版情報：九州大学, 2022, 修士, 修士
バージョン：
権利関係：

Master Thesis

Numerical Simulation of a TLP in Large Waves by OpenFOAM

Marine Environmental Energy Engineering Laboratory
Mechanical and Systems Science and Engineering Major
Department of Integrated Science and Engineering
Interdisciplinary Graduate School of Engineering Sciences
Kyushu University

Li Yansong

Supervisor Prof. HU Changhong

Submission date February, 06, 2023

Contents

Appendix

List of Table

List of Figure

1. Introduction

1.1 Background

The development of renewable energy has become especially important in today's era when onshore resources are increasingly depleted. As a clean and renewable resource, offshore wind energy has attracted more and more attention today. Offshore wind turbines are developed to harvest such offshore wind energy resources. With the development of wind energy to deep water, the research of floating foundations which support wind turbines is particularly important. The fixed platform commonly used in shallow water is no longer applicable in deep water due to high cost, difficulty in construction and installation. In deep water, floating platform is widely used for its, relatively low cost and better performance. A comprehensively lists of the types and examples for floating offshore wind power generation platforms in Japan and abroad can be found in the paper [1].

Tension leg platform (TLP for short) is a kind of platform widely used in floating platforms as shown in Fig 1.1 [2]. It uses residual buoyancy to balance the pre-tension of the tensioned mooring system, which has the characteristics of semi-compliance and semi-rigidity. Therefore, TLP structure can resist the movement caused by waves to provide a relatively stable environment for wind power generation and reduce the impact of variations in Wind Turbine Power on the transmission grid. At the same time, the TLP's own vertical buoy structure also provides a good motion performance for the platform.

Fig. 1.1 Wind power TLP structure

In our Marine Environment and Energy Engineering Laboratory, we are developing a TLP-type floating platform, which can be used as floating offshore electricity transmission tower as shown in Fig.1.2 and Fig.1.3, and ocean environment observation tower. The TLP system will be a low-cost, high-performance offshore floating foundation.

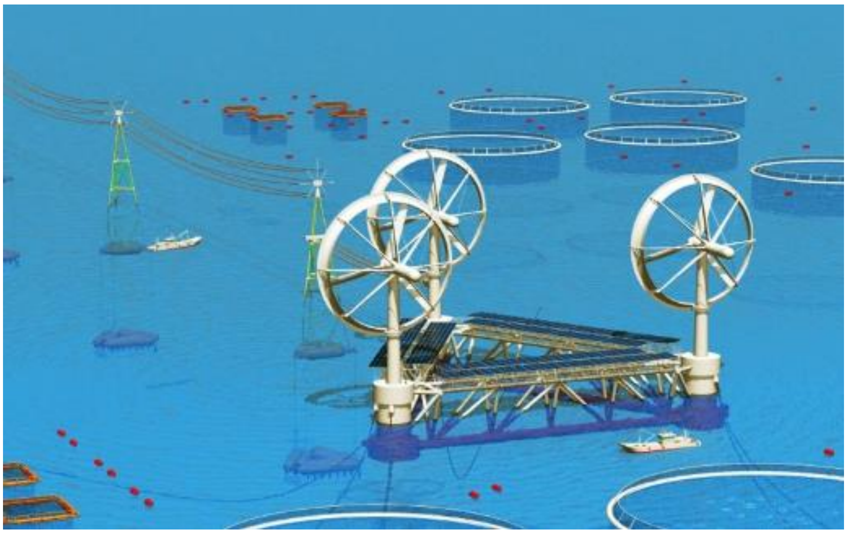

Fig. 1.2 Multi-purpose offshore energy floating platform

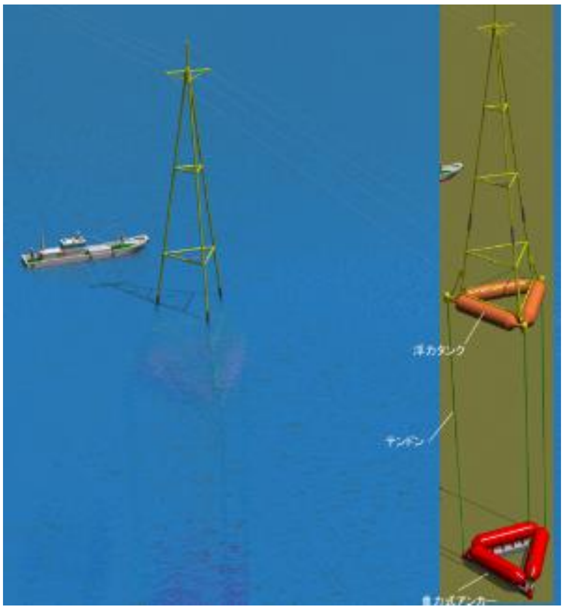

Fig. 1.3 Floating transmission tower

1.2 Research Objective

Floating platforms need to maintain operation in specific sea areas for a long time, so mooring systems are required to provide resilience to restrain movement caused by external loads. On the other hand, the wind turbine platform is not allowed to have a large scale motion response, in order to ensure the normal output power grid of the wind turbine and stabilize it. Since the marine environmental conditions of the wind turbine platform system are very complex when they are put into use under real sea conditions, it is of great significance to study the motion response characteristics of the wind turbine foundation under different sea conditions to guide the design of the wind turbine system, ensure the safety of people and property, and ensure the normal operation of the wind turbine system.

The objective and the key of this research is to use OpenFOAM to study the safety issue of a new type of TLP. This thesis shows the numerical simulation results for the cases under extreme sea conditions. A safety assessment of the TLP is provided based on the numerical simulation results. The present CFD results are also compared with the existing results calculated by a potential flow theory.

1.3 Previous related research

OpenFOAM is a free, open source CFD (computational fluid dynamics, short for CFD) software, which is often used to solve hydro- dynamic problems of ships. At present, many scholars in the world have used OpenFOAM when solving problems related to offshore floating platforms. Agnese Paci et al. develop a numerical wave tank in simulating wave-floating structures interaction [3]. J.H. Chow et al. show the developed solver was brought into test with an experimental floating wind turbine setup on a tensioned leg platform and it has been shown with reasonable validations that the solver was able to capture the wave loads on the floating wind turbine and determine its response [4]. Barajas , G. et al. shows some validation case of TLP simulated by OpenFOAM [5]. Ali Nematbakhsh et al. calculate the effect of wave loads on a wind turbine on a TLP platform by CFD and potential flow theory and compared the results [6]. Naying Wei et al. take a floating system with inclined tension legs as the research object and study its sensitivity to dynamic responses under different loads [7]. Shaoshi Dai et al. evaluate OpenFOAM for use in this field and the simulations were hence performed of the flow field around a full-scale Tension-Leg Platform in steady current at high Reynolds number. A modification that has been shown to improve k-epsilon model's performance in flows [8].

2. Mathematical Model

2.1 Governing Equation

The numerical simulations in this research are based on the continuous incompressible viscous fluid. The governing equation are the continuity equation:

$$\nabla \cdot \boldsymbol{u} = 0 \tag{1}$$

And the Navier–Stokes equations for the momentum evolution:

$$\frac{\partial \boldsymbol{u}}{\partial t} + (\boldsymbol{u} \cdot \nabla)\boldsymbol{u} = \nu \nabla^2 \boldsymbol{u} - \nabla \left(\frac{p}{\rho}\right) + g \tag{2}$$

where **u** is the velocity vector, $\nu = \frac{\mu}{\rho}$. For incompressible fluids, the density ρ of the fluid does not change with time and μ, p, g are representing the viscosity, density, and pressure. ν is called the kinematic viscosity. For detailed equation derivation, please refer to the literature [9].

Reynolds number (Re) are an important dimensionless quantity in fluid mechanics. Reynolds number helps predict flow patterns in different fluid flow situations by measuring the ratio between inertial and viscous forces. At low Reynolds number, flows tend to be dominated by laminar flow which are smooth and streamlined, while at high Reynolds number flows tend to be turbulent which are irregular and chaotic, If the Reynolds number is small, the influence of turbulence can be ignored, and the laminar flow model can be used to improve the calculation efficiency. Let L be a characteristic length dimension (m), Reynolds number can be defined as:

$$Re = \frac{uL}{\nu} = \frac{\rho u L}{\mu} \tag{3}$$

In this research, the VOF (volume of fluid) method is used to capture the free surface. In computational fluid dynamics, the VOF method is a free-surface modelling technique. It is a numerical technique for tracking and locating the free surface (or fluid–fluid interface). It belongs to the class of Eulerian methods which are characterized by a mesh that is either stationary or is moving in a certain prescribed manner to accommodate the evolving shape of the interface.

In OpenFOAM, the multiphase flow problems is solved by interFoam solver [10]. The solver solves the Navier Stokes equations for two incompressible, isothermal immiscible fluids. That means that the material properties are constant in the region filled by one of the two fluid except at the interphase. The density ρ is defined as follows:

$$\rho = \alpha\rho_1 + (1 - \alpha)\rho_2 \tag{4}$$

where α is 1 inside fluid 1 with the density ρ_1 and 0 inside fluid 2 with the density ρ_2. At the interphase between the two fluids α varies between 0 and 1.

The surface tension $f_{\sigma i}$ is modelled as continuum surface force. It is calculated as follows:

$$f_{\sigma i} = \sigma\kappa \frac{\partial\alpha}{\partial x_i} \tag{5}$$

σ is the surface tension constant and κ the curvature. The curvature can be approximated as follows:

$$\kappa = -\frac{\partial n_i}{\partial x_i} = -\frac{\partial}{\partial x_i}\left(\frac{\partial_\alpha/\partial x_i}{|\partial_\alpha/\partial x_i|}\right) \tag{6}$$

To know where the interphase between the two fluids is, an additional equation for α must be solved.

$$\frac{\partial\alpha}{\partial t} + \frac{\partial(\alpha u_i)}{\partial x_j} = 0 \tag{7}$$

The equation is the conservation of the mixture components along the path of a fluid parcel.

2.2 Turbulence Modelling

Considering the situation of simulating extreme ocean waves, the waves will generate local small eddies, and the waves will break up, and some fluids around the floating body will move irregularly. The flow phenomena associated with such wave-body interaction problems are generally turbulent, in this study, the Reynolds-averaged Navier-Stokes (RANS) models are considered for modeling of the turbulence. OpenFOAM includes Reynolds Averaged Simulation turbulence closures based on linear and non-linear eddy viscosity models and Reynolds stress transport models. In the following, the standard k-epsilon (k - ϵ) model is described [11].

The turbulent kinetic energy equation, k:

$$\frac{D}{Dt}(\rho k) = \nabla \cdot (\rho D_k \nabla k) + P - \rho\epsilon \tag{8}$$

Where k is turbulent kinetic energy(m^2s^{-2}), D_k is effective diffusivity for k, P is turbulent kinetic energy production rate(m^2s^{-3}), ϵ is turbulent kinetic energy dissipation rate(m^2s^{-3}).

The turbulent kinetic energy dissipation rate equation, ϵ:

$$\frac{D}{Dt}(\rho\epsilon) = \nabla \cdot (\rho D_\epsilon \nabla_\epsilon) + \frac{C_1\epsilon}{k}\left(P + C_3\frac{2}{3}k\nabla \cdot \boldsymbol{u}\right) - C_2\rho\frac{\epsilon^2}{k} \tag{9}$$

Where D_ϵ is Effective diffusivity for ϵ, C_1 and C_2 is Model coefficient.

The turbulent viscosity equation, ν_t:

$$\nu_t = C_\mu \frac{k^2}{\epsilon} \tag{10}$$

Where C_μ is Model coefficient for the turbulent viscosity, ν_t is Turbulent viscosity.

The model coefficients are C_μ=0.09, C_1=1.44, C_2=1.92, σ_k=1.0, σ_ϵ=1.3.

For isotropic turbulence, the turbulent kinetic energy can be estimated by:

$$k = \frac{3}{2}\left(I\left|\boldsymbol{u}_{ref}\right|\right)^2 \tag{11}$$

Where I is Turbulence intensity(%), u_{ref} is a reference flow speed(ms^{-1})

For isotropic turbulence, the turbulence dissipation rate can be estimated by:

$$\epsilon = \frac{C_\mu^{0.75} k^{1.5}}{L} \tag{12}$$

Where C_μ is a model constant equal to 0.09 by default, L is a reference length scale(m).

2.3 Dynamic Mesh

To simulate the movement of the platform, it is necessary to continuously change the calculation grid to adapt to the influence of the structure movement on the flow field. In this research, the dynamicFvMesh dynamic mesh technology is applied. The solver is sixDoFRigidBodyMotion. When the platform is displaced, the shape of the grid is changed by moving nodes while keeping the topological relationship between each grid node and its neighbors unchanged. In dynamic meshes specifically when working with moving or deforming bodies, the integral form of the general transport equation is written as follows [12]:

$$\int_{V_p} \frac{\partial \rho\phi}{\partial t} dV + \int_{V_p} \nabla \cdot \left[\rho\phi\left(\boldsymbol{u} - \boldsymbol{u}_g\right)\right] dV - \int_{V_p} \nabla \cdot \left(\rho \Gamma_\phi \nabla\phi\right) dV = \int_{V_p} S_\phi \phi dV \tag{13}$$

in the FVM where u_g is mesh velocity, ϕ is transported quantity, volume dV is a function of time. The time derivative can be written as follows:

$$\frac{\partial}{\partial t} \int_{V_p} \rho\phi dV = \frac{(\rho\phi V)^{n+1} - (\rho\phi V)^n}{\Delta t} \tag{14}$$

where n and n+1 denote the respective quantity at the current and next time level.

2.4 Wave Generating

One of the most significant environmental factors affecting the movement of marine engineering structures is the wave. In fluid dynamics, a Stokes wave is a nonlinear and periodic surface wave on an inviscid fluid layer of constant mean depth. The present simulation uses the second-order Stokes wave. In OpenFOAM, the regular wave height is modelled represented by the equation [13]:

$$\eta = \frac{H}{2} cos(kx - \omega t + \phi) + k\frac{H^2}{4}\frac{3-\sigma^2}{4\sigma^3} cos\big(2(kx - \omega t + \phi)\big) \tag{15}$$

where H is wave height, k is wave number, ω is angular frequency, σ is radian wave frequency, ϕ is phase shift, t is time.

2.5 Tension Leg System Simulation

The spring simulation method is used to simulate the vertical mooring system of TLP. The specific implementation utilizes the restraints module in dynamicMeshDict. In the spring simulation method, the vertical mooring system of TLP is equivalent to a spring that can only be stretched but cannot be compressed and does not consider the gravity of the spring itself and the force of the flow field. The spring simulation method is widely used in the motion response calculation of TLP platforms [14].

The basic principle of the spring simulation method is Hooke's law:

$$F = k\Delta l \tag{16}$$

$$E = \frac{stress}{strain} = \frac{F/S}{\Delta l/L} \tag{17}$$

Where k is Elastic coefficient of the spring, E is Elastic modulus.

The k is given in dynamicMeshDict, F is the restoring force provided by the mooring system to the floating structure, and the elongation of the spring is recorded as Δl, which is the difference between the actual length of the mooring line (in the program, that is, the distance between the mooring point and the anchoring point) and the initial length of the mooring line.

3. Computational Model

3.1 TLP Structure

In this research numerical simulation is performed on the motion of the floating platform in different waves, the specific structural part is similar to the part circled in the figure 3.1 shown as below [15], but the structural parameters are different from the figure and the underwater structure is similar to the figure 3.2 shown as below [16].

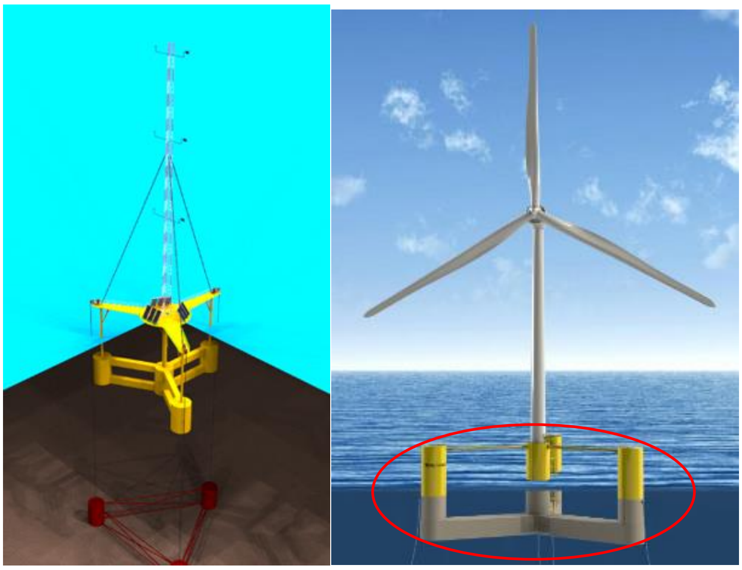

Fig. 3.1 Platform structure for simulation

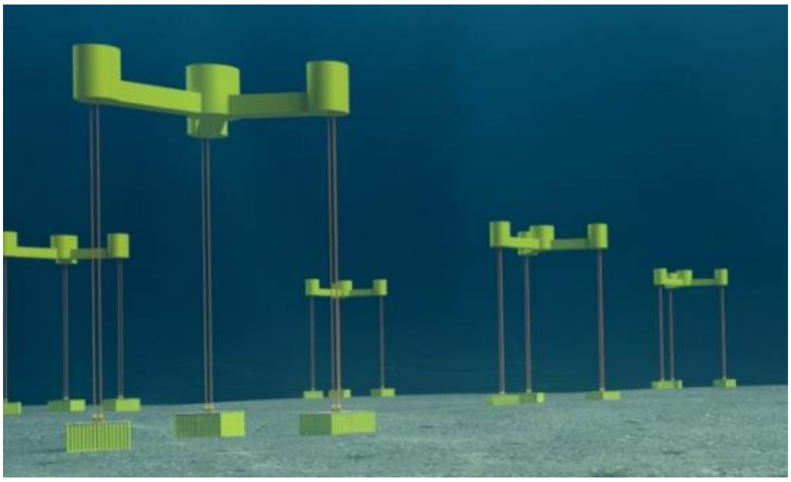

Fig. 3.2 TLP underwater structure

The structure composed of the platform and the tension leg structure considered in this research is shown in Figure 3.3. The TLP acts as a floating foundation and consists of a central column and three vertical buoys. The layout of the calculation domain is shown in Figure 3.4. Half of the structure are submerged in the mean sea level, the draft is 10 meters, and the sea depth in the simulation is set to 100 meters. In order to save calculation time in this simulation, the water depth drawn in the calculation domain is 50 meters, but the result is correspondent to the result of 100 meters of water depth. In the simulation, the origin of the coordinate axes is set at the center of the water surface line of the TLP, the z-axis is vertically upward, and the wave propagates toward the positive axis of the x-axis. The water depth is 100 meters, the wave period is 15.8 seconds. According to the linear wave theory, the wavelength is 365.3 meters. The computational domain is 800 meters long, 40 meters wide, and 90 meters high. Because the wavelength is very long, the calculation domain needs to have a large length in the wavelength direction.

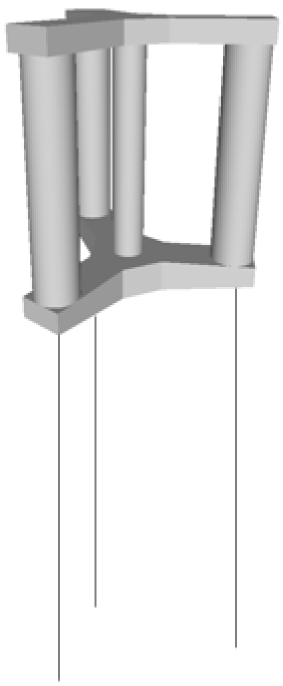

Fig. 3.3 TLP structure

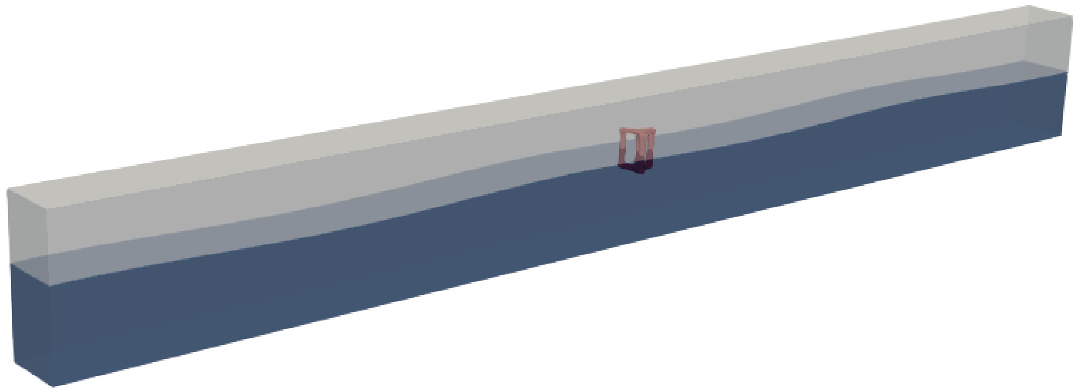

Fig. 3.4 Calculation domain

The main parameters of the tension leg system that restricts the movement of the platform are shown in Table 1. There are three sets of tension legs, and each set of tension legs is moored outside the lower edge of the three vertical buoys on the platform. The main parameters of the TLP platform are shown in Table 2.

Tab. 1 Main parameters of mooring system

Characteristic	Parameter
Number of tension legs	3
Connection point to the platform center/m	12
Tendon length/m	88
Tendon weight/kg	0
Tendon axial stiffness/$(N \cdot m^{-1})$	22840909
Tendon total pretension/N	4.5×10^6

Tab. 2 Main parameters of platform

Characteristic	Parameter
Total mass/kg	3.9×10^5
Total displacement/ton	828
Diameter of column/m	3
Diameter of buoy/m	4
Column and buoy height/m	20
Center distance between buoy and column/m	10
Bottom plate thickness under column/m	3
Bottom plate thickness under buoy/m	2
Side length of the bottom regular hexagon/m	4
Center of mass at rest/m	(0.0, 0.0, -6.8)
Center of rotation at rest/m	(0.0, 0.0, 0.0)
Center of gravity moment of inertia/(kg·m^2)	2.718×10^7, 4.386×10^7, 4.386×10^7

3.2 Mesh Generation

In order to ensure that waves can be accurately generated and propagated stably in the numerical simulation, and to capture the internal changes of the flow field and the free surface changes of the flow field, etc., it is necessary to generate grids for the inside of the flow field and the surface of structures, and to refine the grids in some areas. Use the snappyHexMesh [17] tool to generate mesh, which can capture the boundary conditions of the object surface and refine the background mesh to generate a high-quality grid. The specific process is as follows: firstly, extract the feature edges of the platform model, and refine mesh on the free surface range and the platform surface for more accurate capture. The calculation domain mesh is shown in Figure 3.5, and the TLP platform surface and nearby grids are shown in Figure 3.6 and Figure 3.7. The number of grids in the simulation is about 7 million. The larger the simulated wave height, the larger the range of free surface should be refined, so the larger the grid amount. At the same time, the setWave tool is also used to give the free surface in the simulation a generated wave at zero time to reduce the time required for the wave to propagate to the floating platform and reduce the burden of simulation calculations.

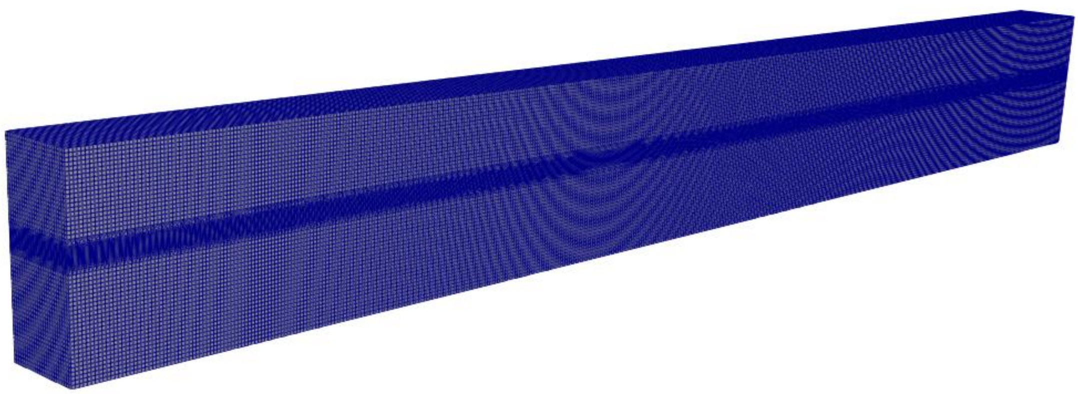

Fig. 3.5 Calculation mesh

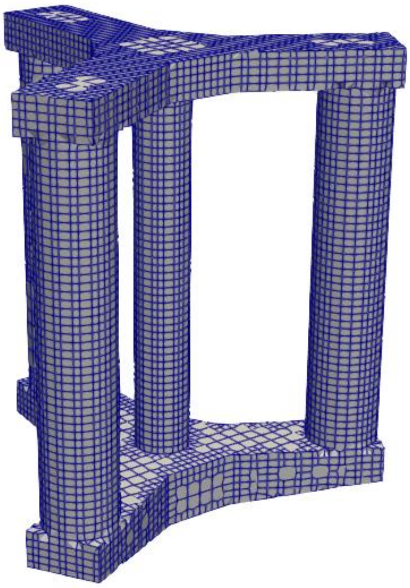

Fig. 3.6 Mesh on the surface of platform

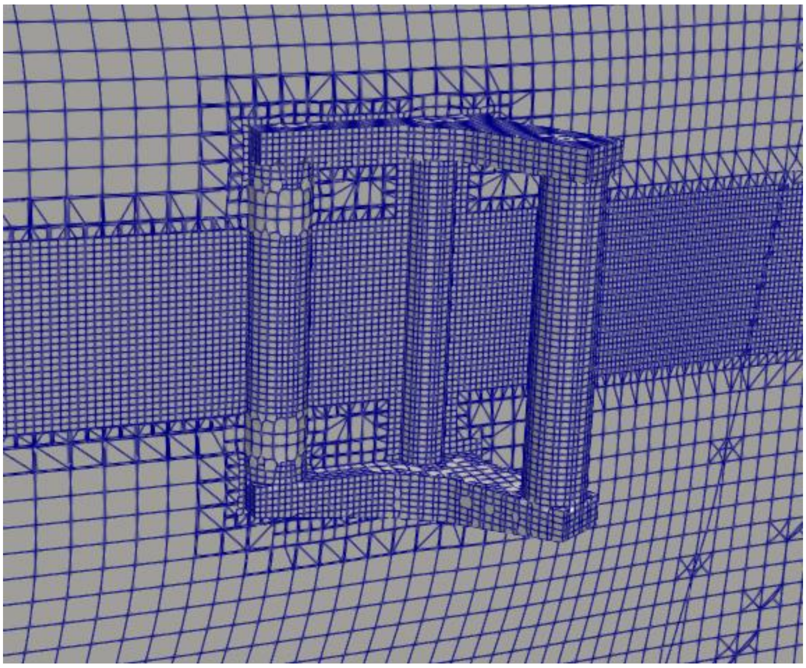

Fig. 3.7 Mesh near the surface of platform

3.3 Validation Case

Validation is made by using a benchmark to verify the accuracy and reliability of the interFoam solver and dynamic mesh solver. These two solvers can solve problems like floating body in a wave. For specific experimental parameters and operation methods, please refer to article [18] [19], which uses CIP method to model nonlinear interactions between extreme waves and a floating body.

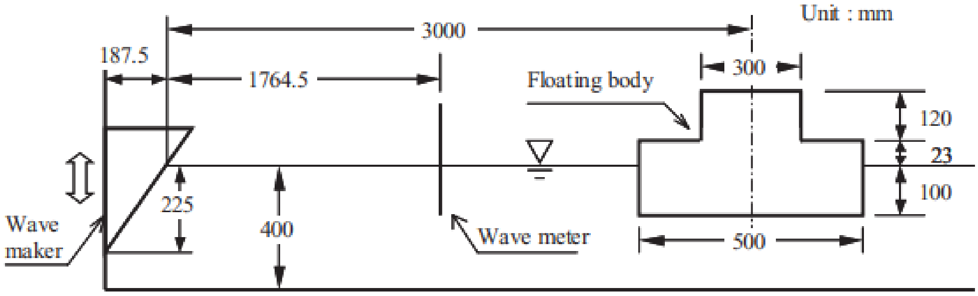

Fig. 3.8 Schematic view of 2-D

Figure 4.1 shows the parameters of the validation case. Use the same simulation parameters, but use interFoam and dynamic mesh solver to solve the problem to observe the calculation results

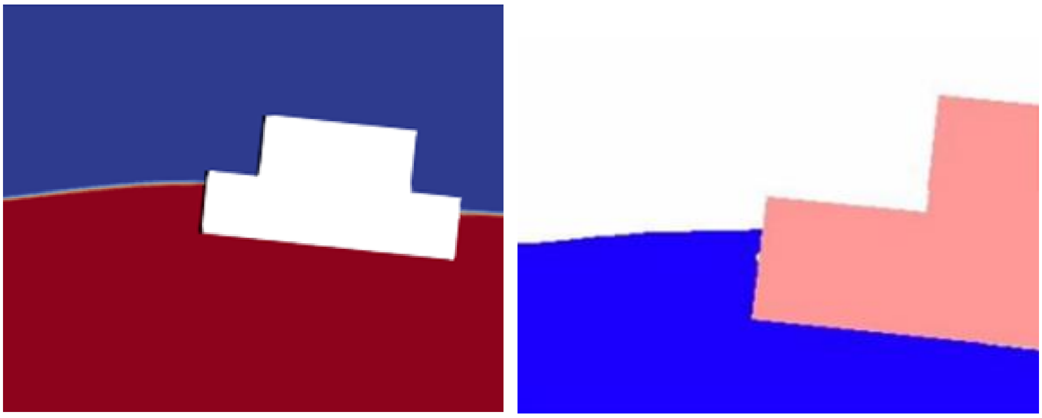

Fig. 3.9 Snapshot at the same time in simulation

On the left of figure 4.2 shows the results from interFoam solver, the right comes from the article. For other comparison results, please see the figure below.

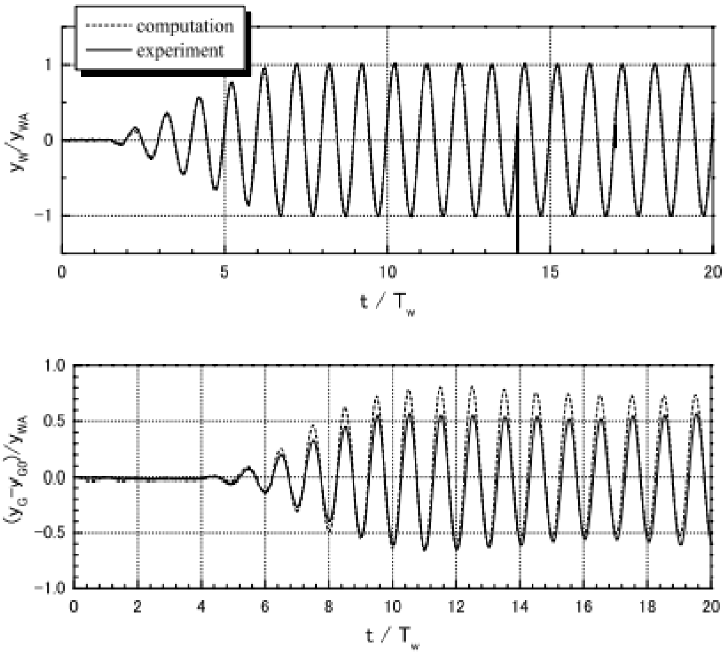

Fig. 3.10 Results from paper

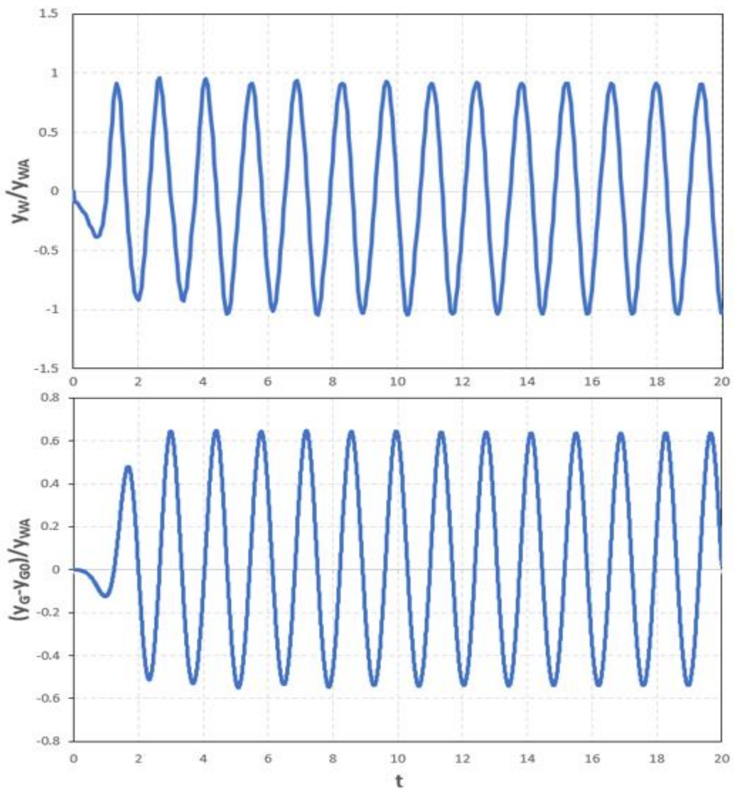

Fig. 3.11 Results used by interFoam

These two figures respectively show the wave elevation and body motion in vertical way under the time series. The simulation results are in good agreement with the literature results, proving that the interFoam solver the reliability of modeling such problems.

4. Simulation Results and Analysis

4.1 6DoF Results of TLP

To study the motion characteristics of the platform in the wave field, give the wave field a formed wave at the initial moment in order to reduce the time required for calculation. This paper simulates ten wave periods of about 160 seconds. Select enough simulation time to ensure that the motion of the platform tends to be stable and reduce the data inaccuracy caused by fluctuations. The following will analyze the 6DoF(six-degree-of-freedom) motion response of TLP under extreme waves.

The time-history curves of different degrees of freedom movement, platform force, and mooring tension are obtained. The CFD simulation results are compared with the existing results. In this paper, the six degrees of freedom motion responses, surge, sway, heave, pitch, roll, and yaw are discussed. The following table 3 shows the statistics of TLP motion response under extreme sea conditions with a significant wave height of 10 meters.

Tab. 3 TLP motion response statistics under extreme sea conditions

	Surge/m	Sway/m	Heave/m	Roll(°)	Pitch(°)	Yaw(°)
Max	11.35	0.078	0.15	0.14	0.27	0.49
Min	-10.37	-0.17	-1.65	-0.020	-0.11	-0.36
Average	3.06	-0.021	-0.78	0.027	0.018	0.076
σ	7.36	0.048	0.52	0.032	0.065	0.16
rms	7.97	0.052	0.94	0.042	0.067	0.18

In the table, σ represents the standard deviation, which is a measure of statistical distribution degree, reflecting the dispersion degree of a data set. Rms represents the root mean square, which is used to measure the deviation between the observed value and the true value.

Due to the action of waves, among the 6 degrees of freedom motion, the surge motion is the most significant, the motion amplitude is the largest, and the fluctuation is the most violent. Due to the symmetry of the mooring system and environmental conditions, the amplitudes of sway and yaw movements are also small.

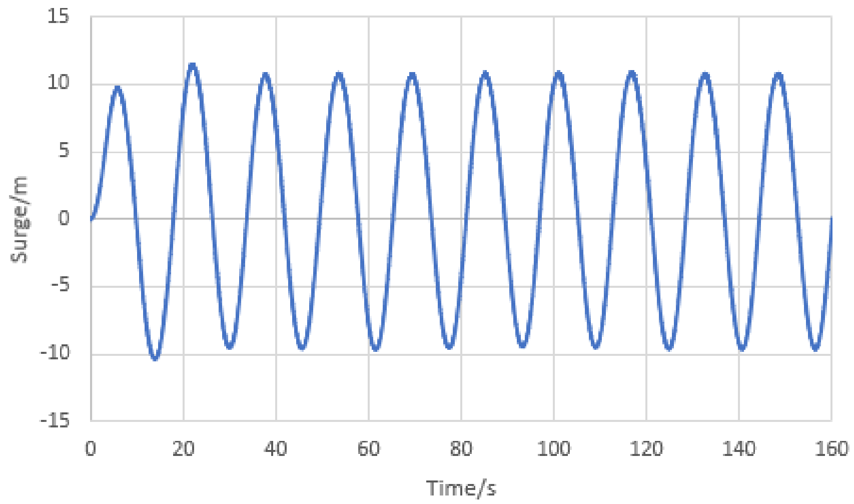

Fig. 4.1 Surge time-history curve under extreme waves

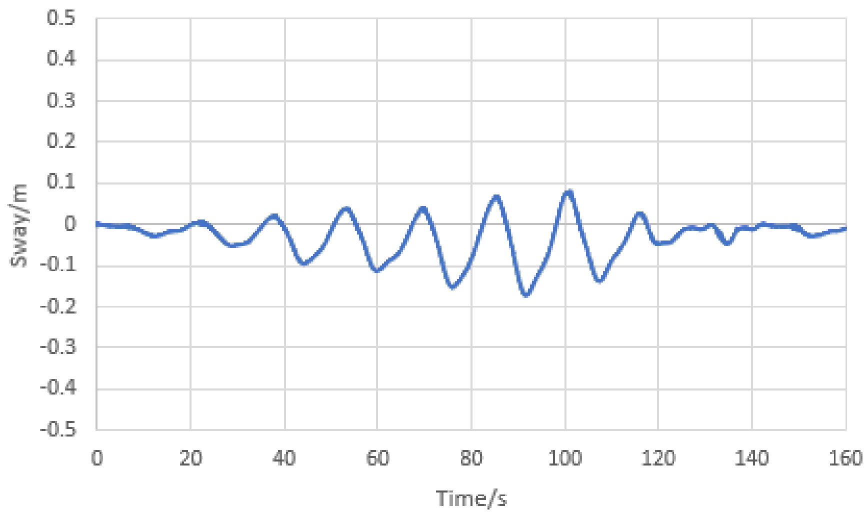

Fig. 4.2 Sway time-history curve under extreme waves

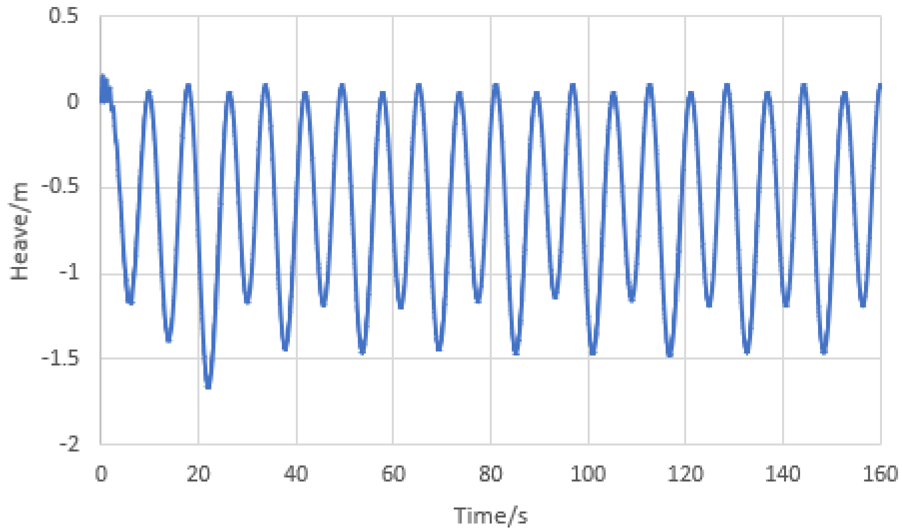

Fig. 4.3 Heave time-history curve under extreme waves

From the analysis of the time-history curves of the surge, sway and heave of the TLP platform in the above figures, it can be known that the amplitude of the surge motion is relatively large, while the amplitude of the pitch and heave motion is relatively small. The surge motion is mainly the result of the wave response, and the motion frequency is mainly dominated by the wave component. The movement range of the sway is relatively small, because the wave simulated in this research is a one-way regular wave, so it has little effect on the sway. Due to the inherent characteristics of the TLP mooring system, the equilibrium position for the heaving motion is below the water level. The main components of the heave motion response of the platform are wave frequency response and surge resonance response. Where wave frequency is dominant. Because the platform is initially in an upright state, the heave and surge will be coupled in motion.

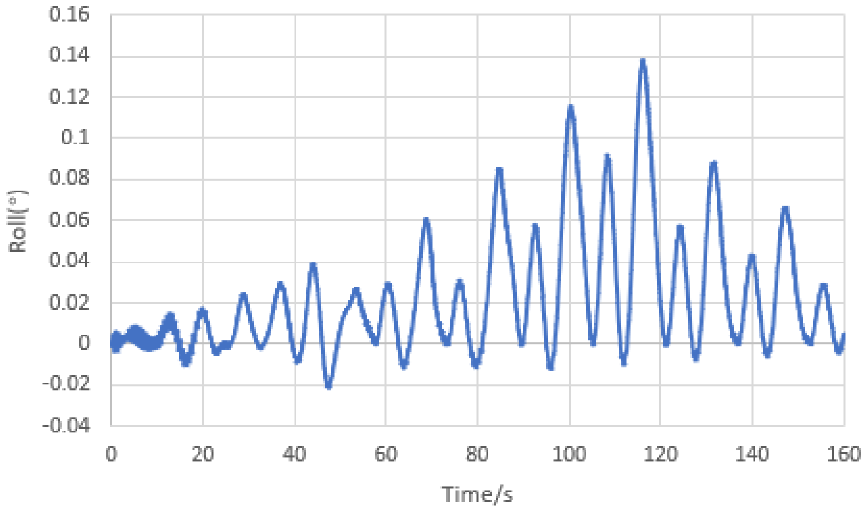

Fig. 4.4 Roll time-history curve under extreme waves

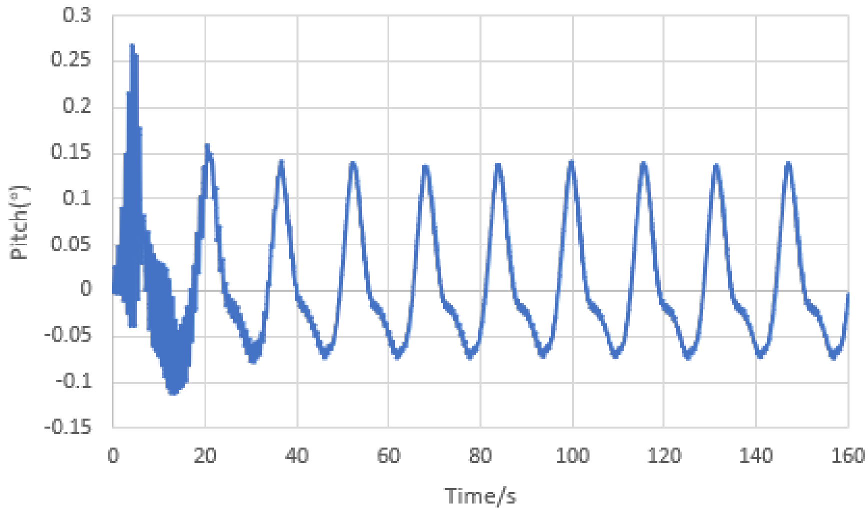

Fig. 4.5 Pitch time-history curve under extreme waves

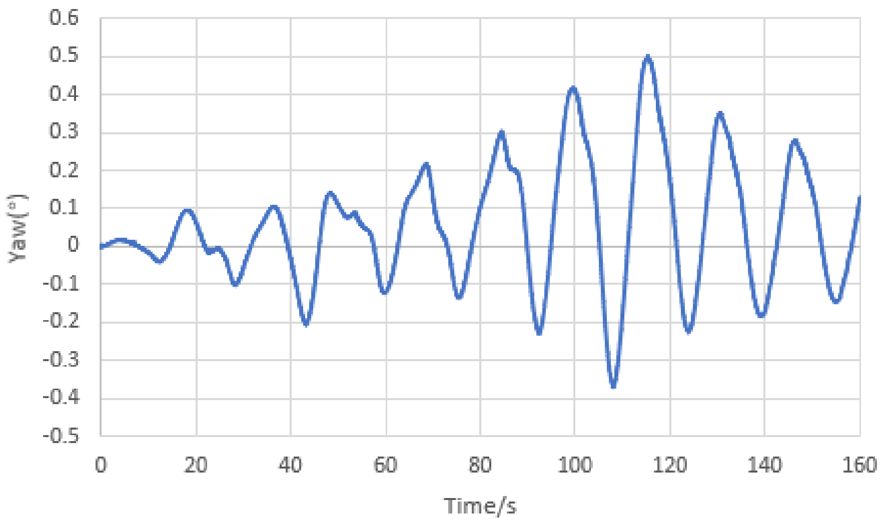

Fig. 4.6 Pitch time-history curve under extreme waves

From the analysis of the time-history curves of roll, pitch and yaw of the TLP platform in the above figures, it can be seen is that the roll and pitch amplitudes are relatively small, and the yaw amplitude is relatively large. This is because of the characteristics of TLP, is approximately flexible in the plane and the out-of-plane is approximately rigid. The time history curves of roll and yaw both show a trend that the maximum value first increases and then decreases within a period. This is due to the relationship of numerical simulation which needs a certain simulation time to ensure the overall motion stability of TLP.

Overall, the heave, roll and pitch movements all have high-frequency vibration phenomenon in the early stage of simulation. As time increases, it will gradually decay and consume. From the above figures, we can know that when the platform encounter extreme sea conditions, the amplitude of the surge motion is relatively large, and the amplitude for the pitch and heave motions is small, which is corresponding to the fact that the TLP is nearly flexible in the plane and nearly fixed outside the plane. The generation of this motion characteristic is determined by the mooring characteristics of TLP itself, and the tension legs of TLP balances the buoyancy force greater than gravity. Therefore, the mooring line is always in tension, which limits the amplitude of out-of-plane motion. The main body of the TLP is an upright buoy, the dimensions in the draft direction are much larger than in the horizontal plane. Therefore, the wave force in the vertical direction is smaller than the wave force in the horizontal direction. Further, it has the characteristics of flexibility in the plane. This characteristic of TLP makes it well resistant to the movement caused by waves and provides a relatively stable environment for wind power generation and power transportation.

4.2 Force Results of TLP

The results of the wave load on the platform and the tension on the mooring system are plotted as time-history curves. Force analysis of the platform helps to understand and evaluate its performances in extreme sea conditions.

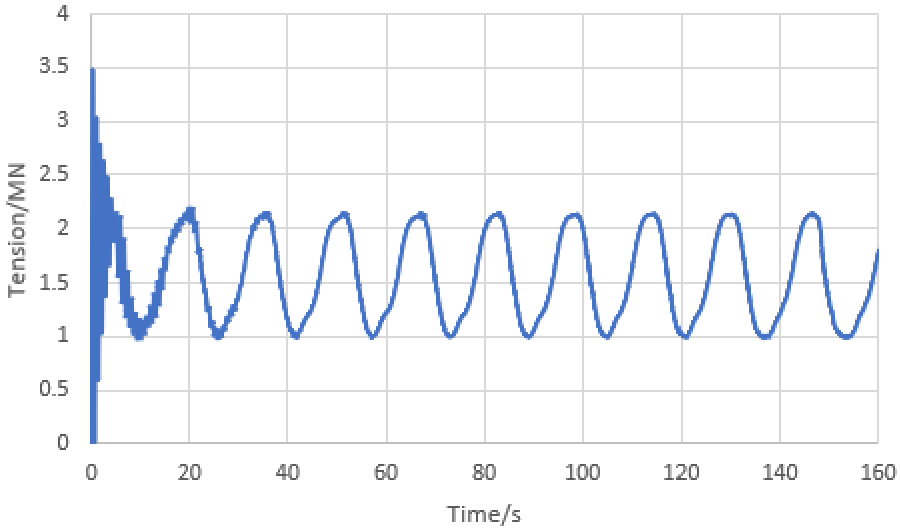

Fig. 4.7 Tension of per tendon

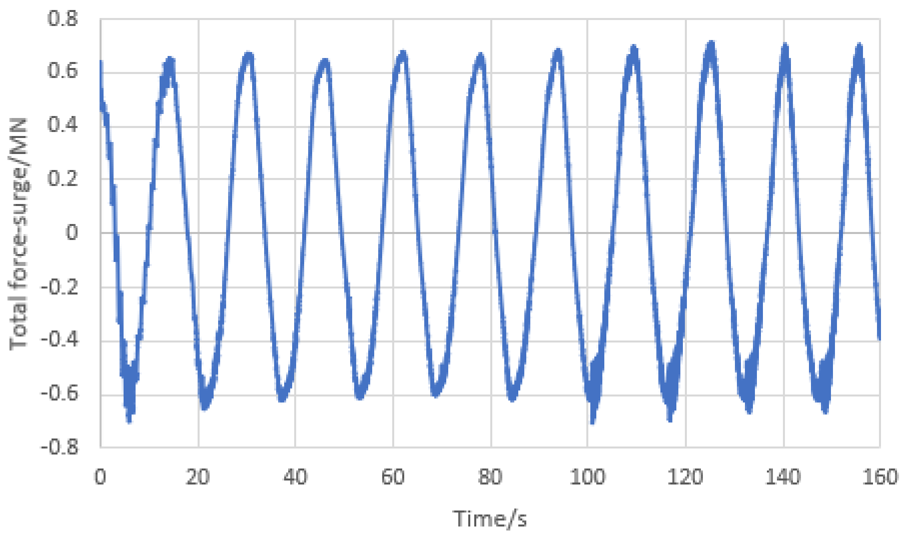

Fig. 4.8 Force in the surge direction of TLP

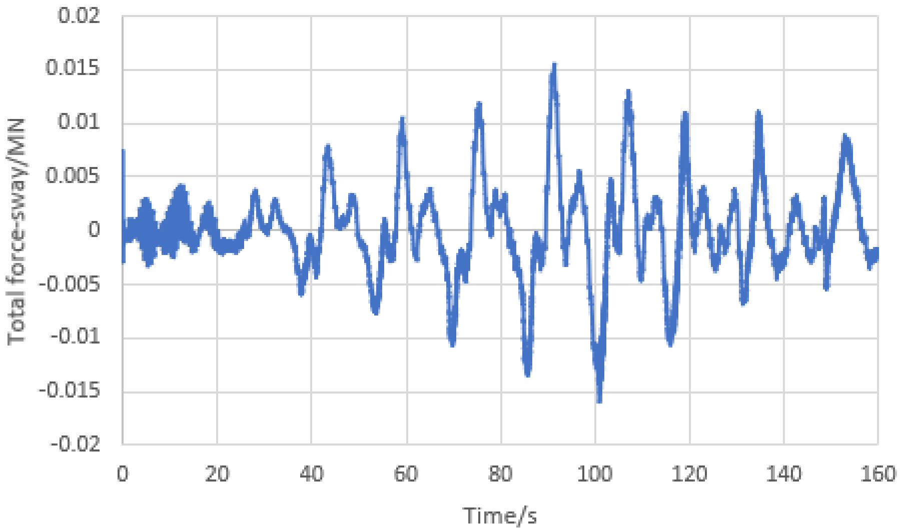

Fig. 4.9 Force in the sway direction of TLP

The figure above shows the time history curves of the total force on the platform in the direction of surge and sway and the tension on the tendon leg. What can be seen is that the tension curve is mainly dominated by the wave frequency, and the force in the sway direction is relatively small. In the following, we will mainly discuss the motion responses in the surge, heave and pitch directions. From the tension leg tension time series curve we can see that the tendon is always under tension. When the calculation is stable, the maximum tension can reach 2.2MN.

Compared with the potential flow theory results, the CFD results can clearly reflect the influence of higher-order components in the wave on the motion performance of the platform and can also visualize the detailed flow field. In order to analyze the wave surface more clearly, the flow field and velocity field near the platform are studied.

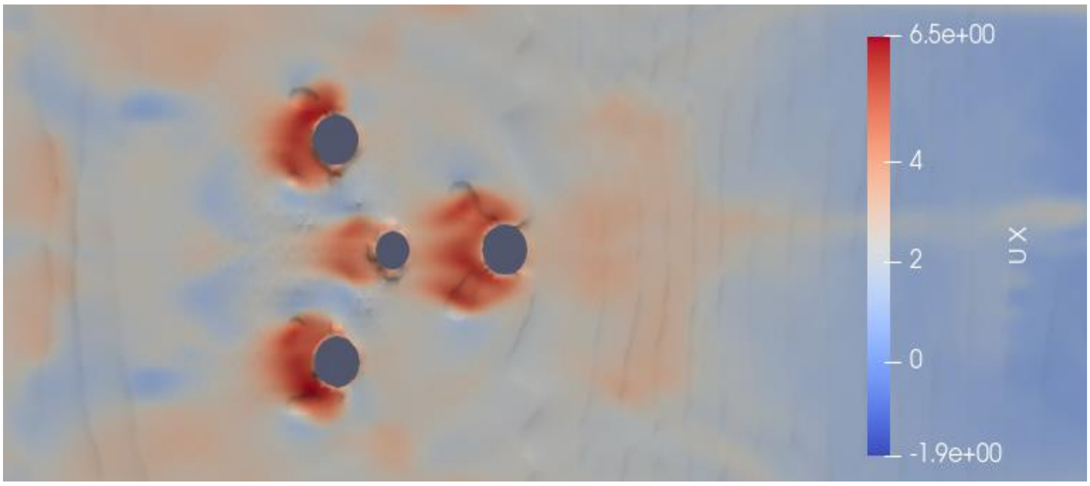

Fig. 4.10(a) Wave velocity at wave crest arriving

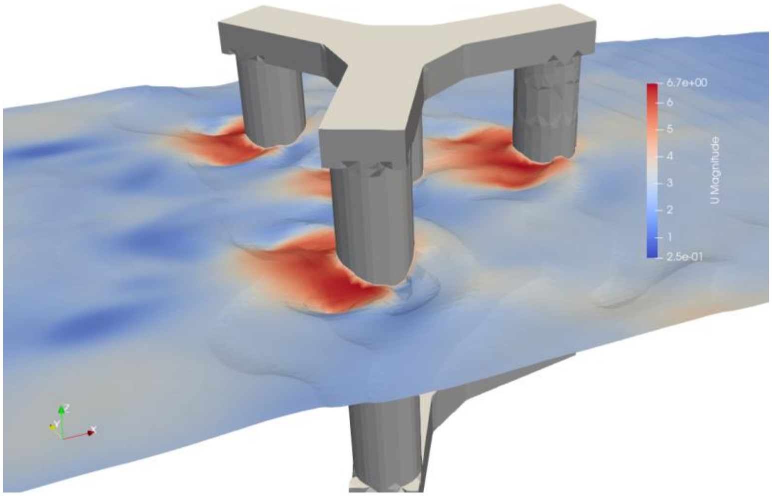

Fig. 4.10(b) Wave velocity at wave crest arriving

The above figure 4.10(a)(b) shows the schematic diagram of the flow field velocity when the wave peak reaches the TLP from two angles. The waves will be blocked as they propagate to the platform column, creating localized secondary waves. When the crest reaches the column, a climbing phenomenon occurs on the column surface.

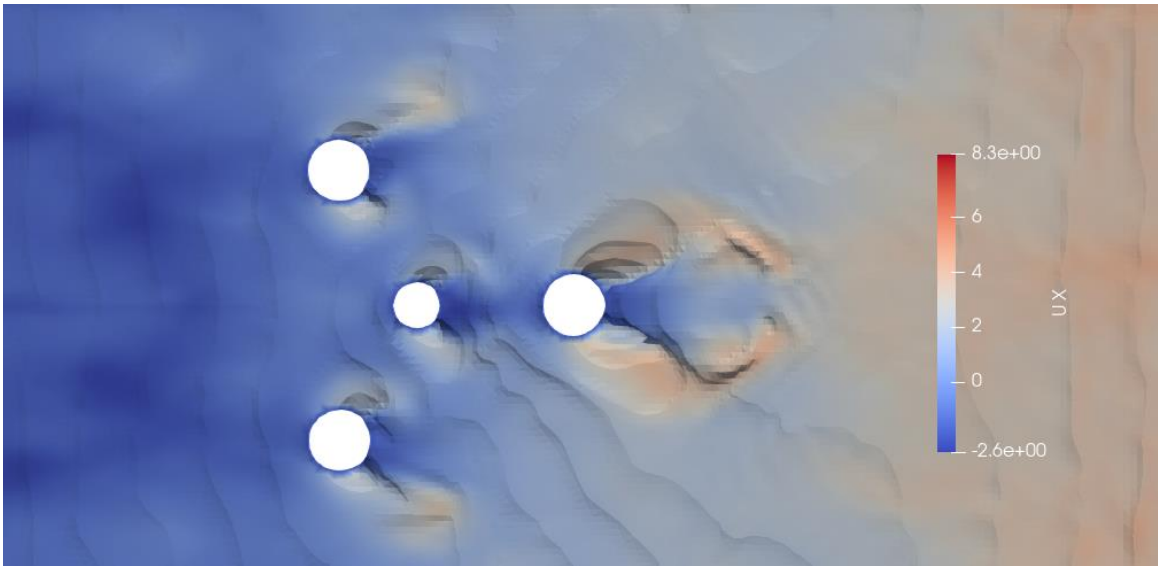

Fig. 4.11(a) Wave velocity at wave crest passing

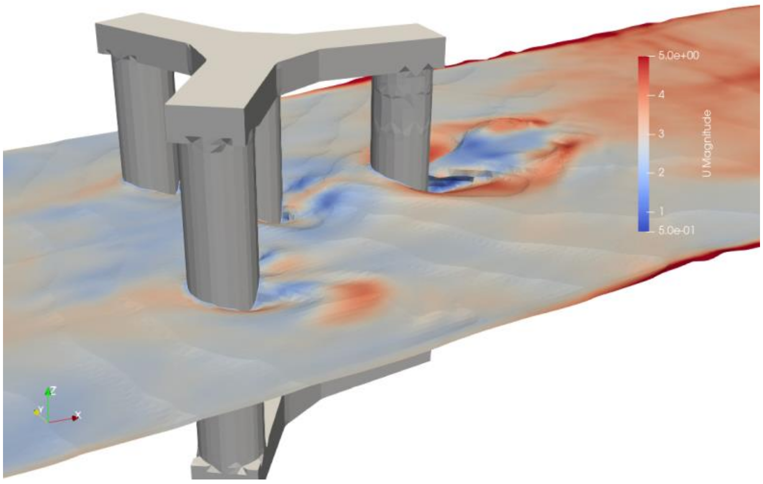

Fig. 4.11(b) Wave velocity at wave crest passing

Figure 4.11(a)(b) shows the schematic diagram of the flow field velocity when the wave crest leaves the TLP from two angles. The wave continues to propagate, the wave blocked by the column leaves, bypasses the column and continues to propagate. Superimposed on the incident wave, the wave deformation occurs.

From the figures we can see that the two-dimensional regular wave used in the simulation, after a certain period of evolution and interaction with the platform, the flow field becomes very complex and the overall wave front is greatly affected. The wave becomes three-dimensional.

It can be seen that due to the blocking effect of the column of the platform, the waves radiate and diffract near the column to form local secondary waves. The analysis of the velocity field shows that the existence of platform column has a great influence on the fluid velocity.

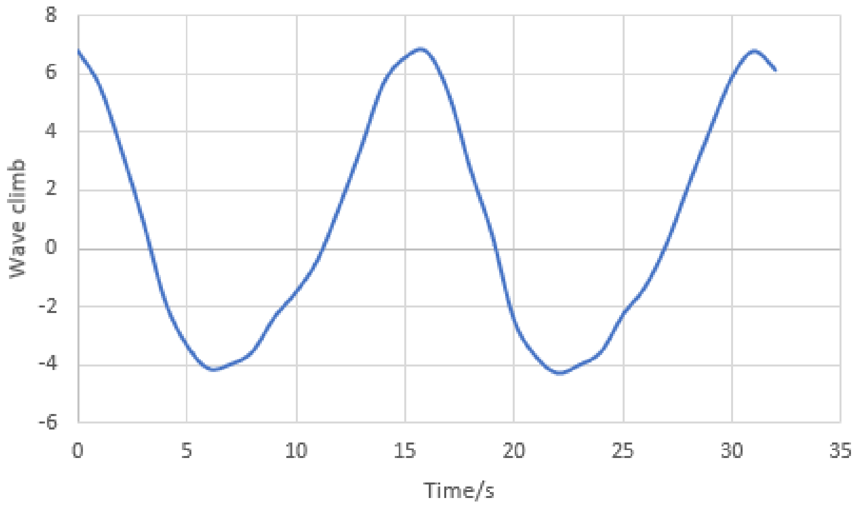

Fig. 4.12 Wave climb in two periods

Figure 4.12 shows the approximate time history curve of the wave climbing height on the buoy of the floating platform. A wave with a wave height of 10 meters can climb to a height of about 7 meters above sea level in the simulation. Given such data can facilitate subsequent numerical simulations to roughly guess the heights of different wave height climbs. A wave height of 16 meters will probably cause the phenomenon of wave on the deck.

4.3 Compared with Potential Theory Result

One of the concerns regarding tension leg platform is the high natural frequencies of the structure that may be excited by nonlinear waves loads. Since Computational Fluid Dynamics (CFD) models are capable for capturing nonlinear wave loads, they can lead to better insight about this concern. However, the results calculated by the potential flow theory do not contain nonlinear wave loads. The results are compared with the results of potential flow theory. Comparing the calculation results of the two can better facilitate us to understand the force and motion of the floating platform under complex sea conditions.

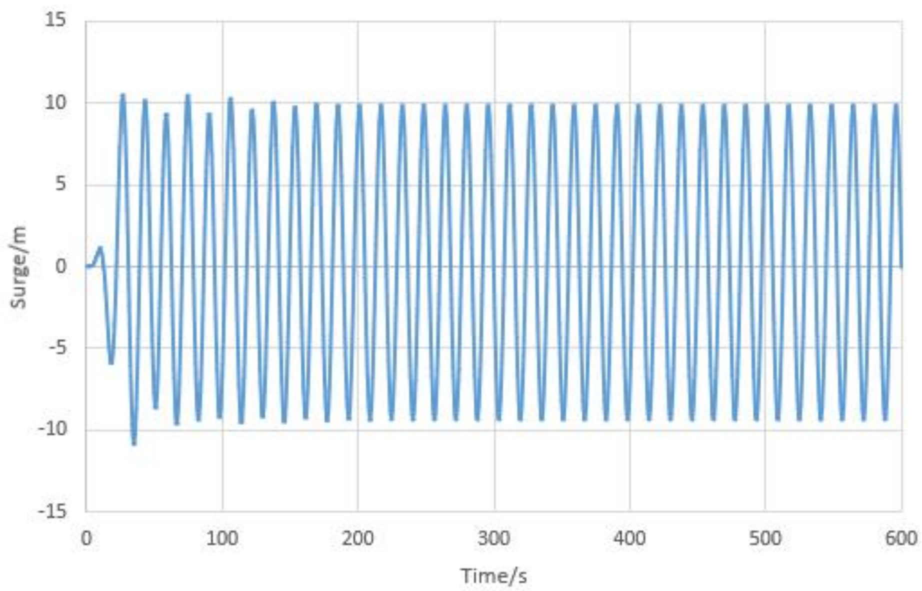

(a)

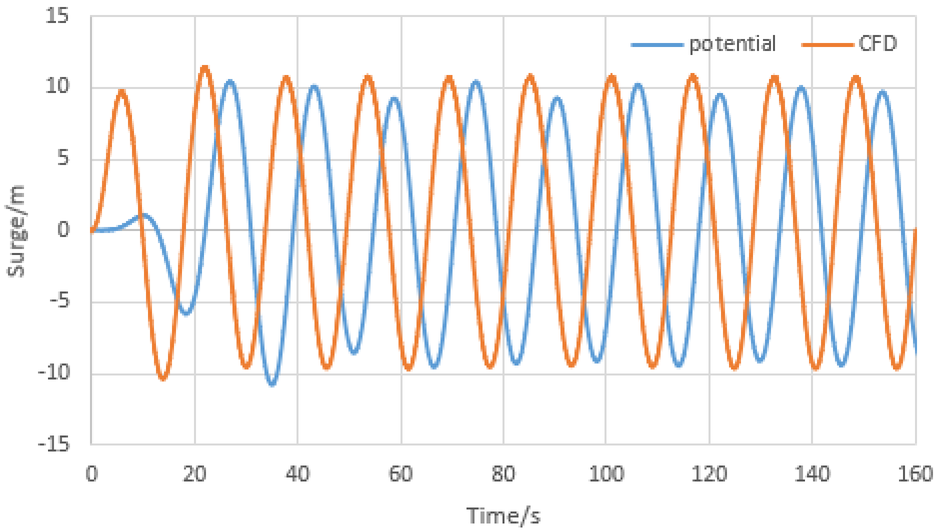

(b)

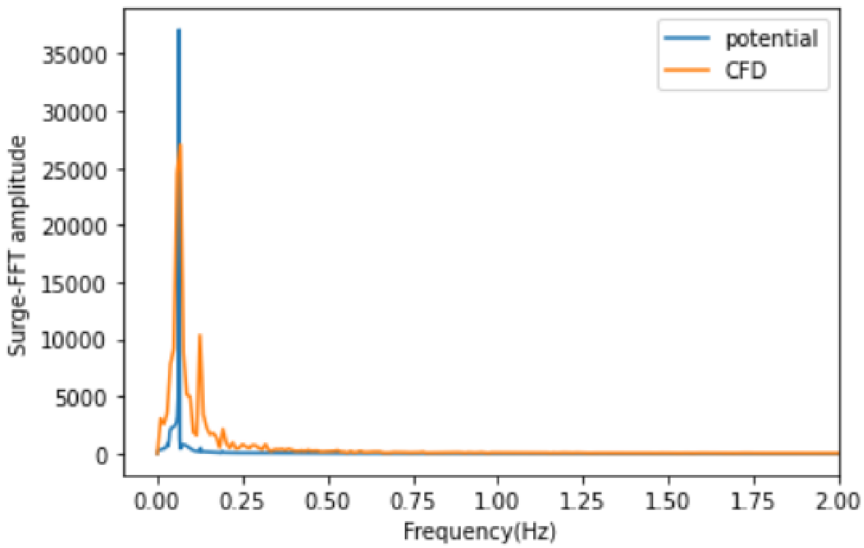

(c)

Fig. 4.13 The surge response compared result and frequency domains.

Figure 4.13(a) shows the surge time curves used by potential flow theory. Figure 4.13(b) is the comparison for easy understanding of the differences between different simulation methods. Figure 4.13(c) shows the Fast Fourier Transform (short for FFT) results, which is a method to transform a signal into the frequency domain, and it is easy to see the characteristics. The code for the FFT is adapted from this web article used by Python [20]. The order shown in figure (a)(b)(c) will not be repeated below. The horizontal axis of the FFT figure is the frequency, and the vertical axis represents the intensity. The results calculated by potential flow theory method and CFD method both show high intensity at the same frequency, which shows that the calculated results are in good consistency. The CFD simulation considers the components of high order of the wave. According to the results of the time history curve and energy spectrum of the surge motion under extreme sea conditions, the frequency response of the wave is the main component in the motion at that time, and the resonance response of the surge is also more obvious. The wave frequency response component is much larger than the surge resonance response. In the CFD simulation, there are more high-order wave components and the energy is more dispersed, so the peak value of the wave frequency component is smaller than the simulation results of the potential flow theory, and the surge resonance response is also more dispersed.

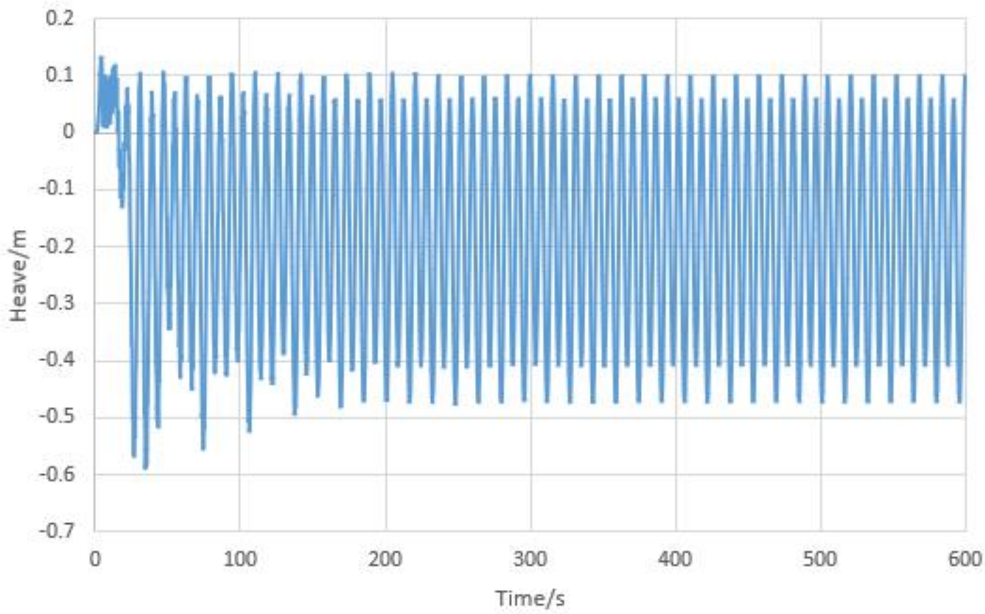

(a)

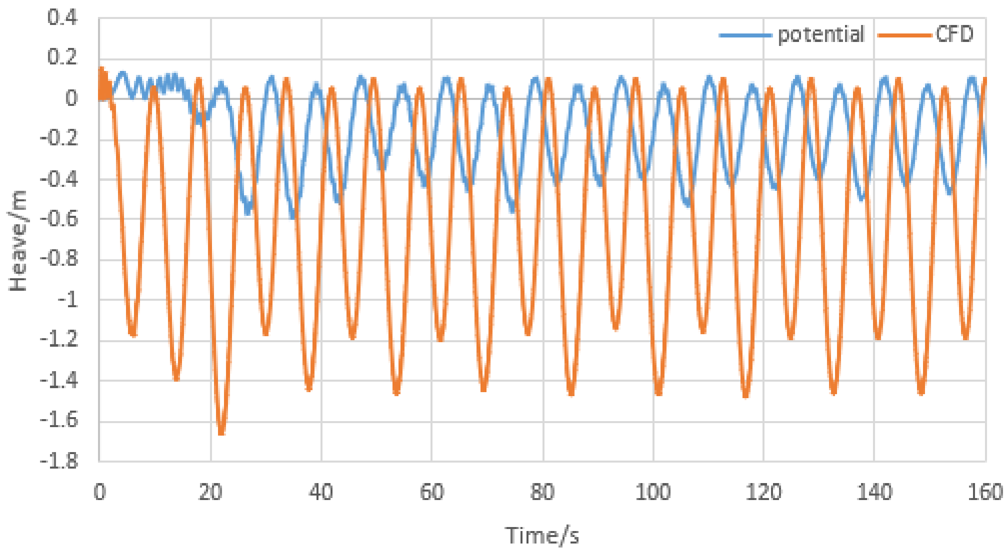

(b)

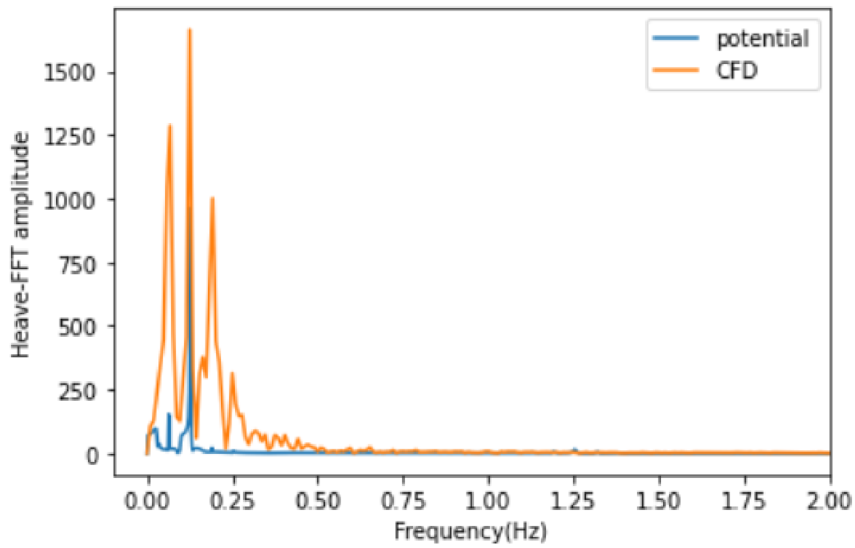

(c)

Fig. 4.14 The heave response compared result and frequency domains.

The time history curve and energy spectrum of the heave motion under extreme sea conditions show that the main components of the heave motion response of the platform are wave frequency response and surge resonance response under extreme sea conditions. Among them, the wave frequency is dominant, because the platform is initially in an upright state, and the heave and surge will be coupled in motion, so the surge resonance component will appear in the energy spectrum. The heave motion due to the heave force on the TLP is very small due to the high stiffness of TLP tendons. If the still water equilibrium position of the TLP is used as the referenced point for measurements, both negative and positive surge motions result in a negative heave motion, which can be seen in both CFD and Potential Flow Theory time domain results.

We can see there is different in heave motion in Figure 4.14 (b). This can be due to better representation of nonlinear effects in the CFD based model, namely by applying the hydrodynamic force at the TLP instantaneous position and by integrating the hydrodynamic loads up to exact free surface. Figure 4.14 (b) also shows nonuniformity in the heave amplitude which is due to the undamped slow transient surge response of the TLP and can be observed in the frequency domain response as a peak at low frequency which is surge natural frequency.

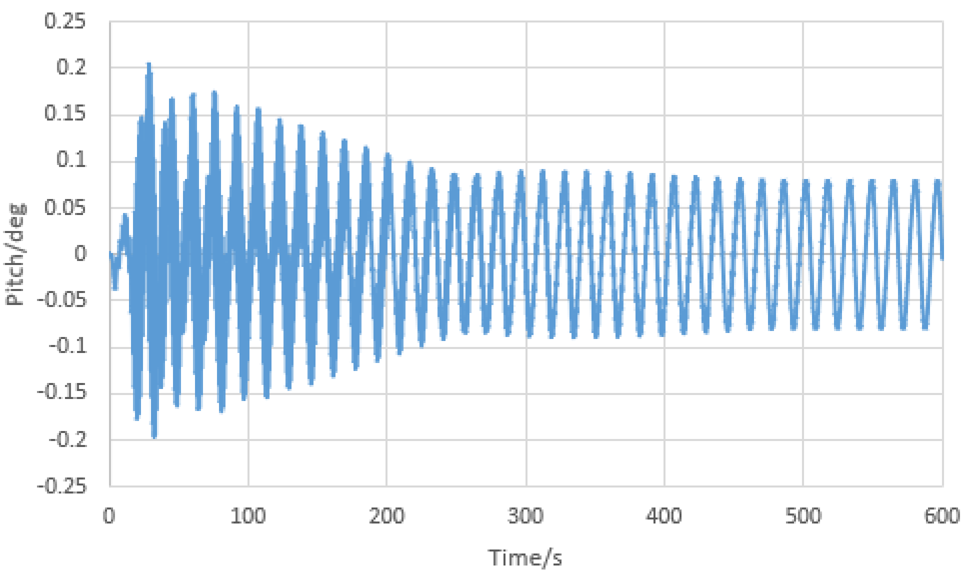

(a)

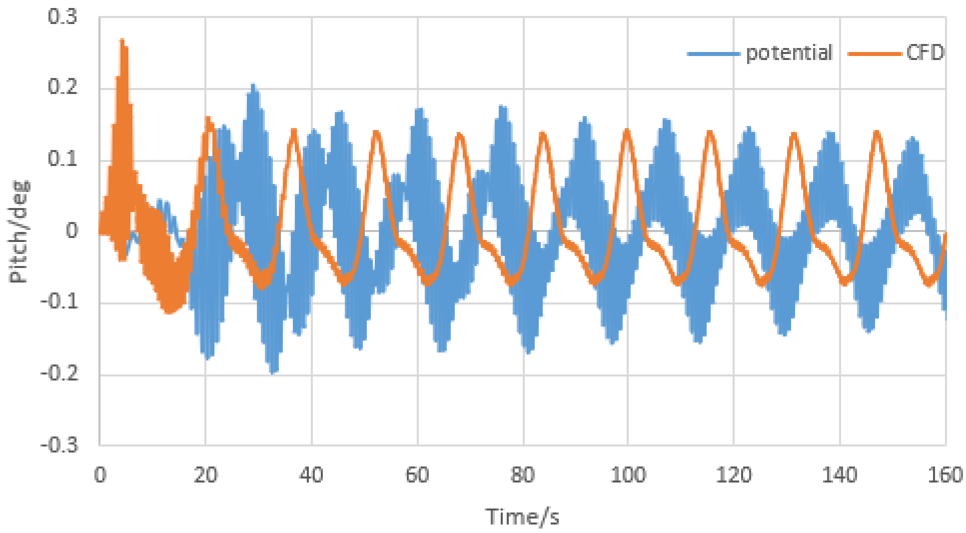

(b)

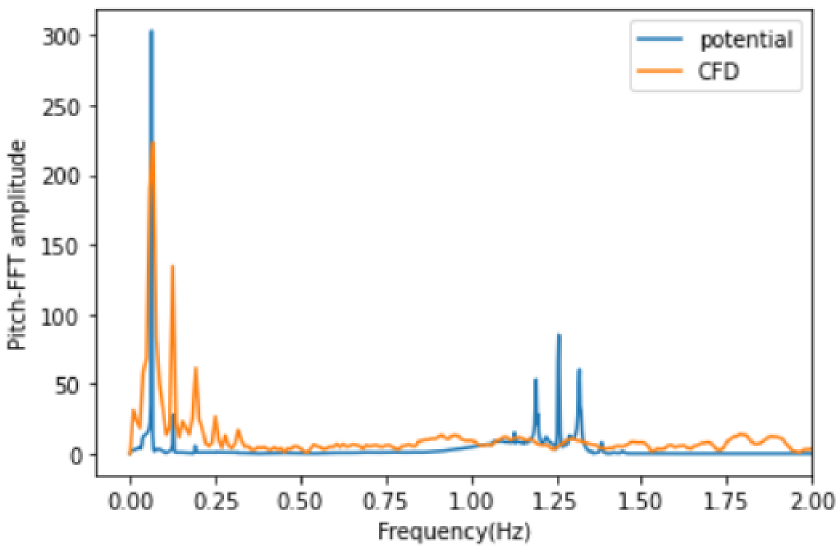

(c)

Fig. 4.15 The pitch response compared result and frequency domains.

Figure 4.15 is the time series curve and energy spectrum of the pitch motion of TLP under extreme sea conditions. Compared with the potential flow theory solution, some high-frequency vibrations observed in the CFD results will gradually decay and dissipate as time continues to grow. However, the potential flow solution needs more simulation time to get stable. That is also what we can see in FFT figure, the potential flow theory results have some peaks near 1.25Hz. More nonlinear components in response can be seen compared with surge and heave. In this case, the dominant components in the energy spectrum are wave frequency response and pitch resonance response components respectively. In the CFD simulation, in addition to the first-order wave components, higher-order wave components can also be seen. It can be seen from the CFD results that the pitch resonance response component of platform motion is due to that the higher-order components in the wave becomes larger, and the frequency range of the response is also larger. From the above analysis, the high-order load of the wave has a great influence on the pitch motion of TLP in this case. This difference in FFT figure peak is due to the difference in the structural (tendons) or hydrodynamic load modeling. In the CFD model, the effects of hull motion for calculating hydrodynamic loads are taken into account while in the potential flow theory model the hydrodynamic loads are applied at the TLP mean position. This relative motion allows the TLP to follow the wave and may cause lower moment on the TLP.

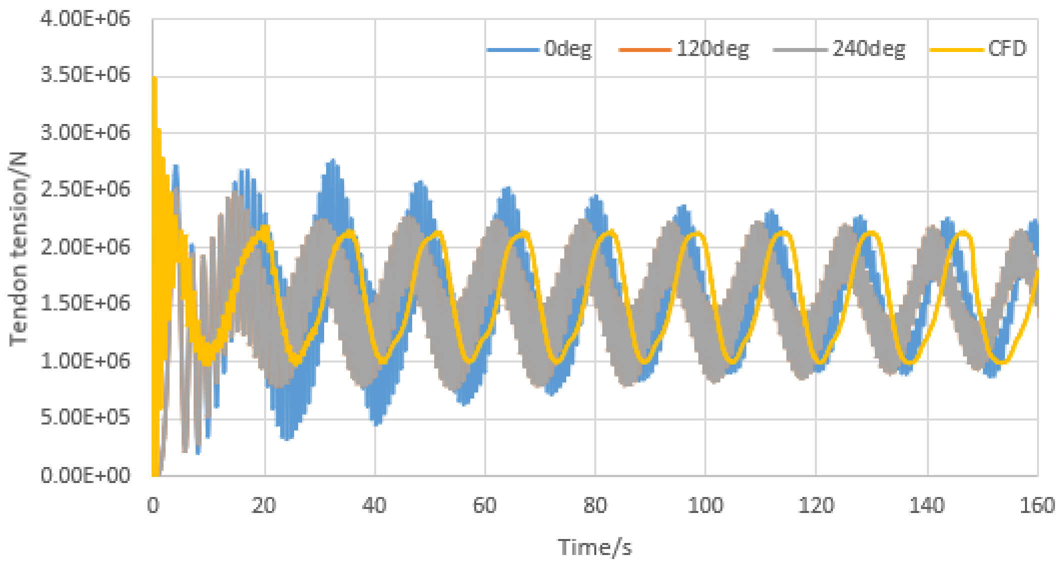

(a)

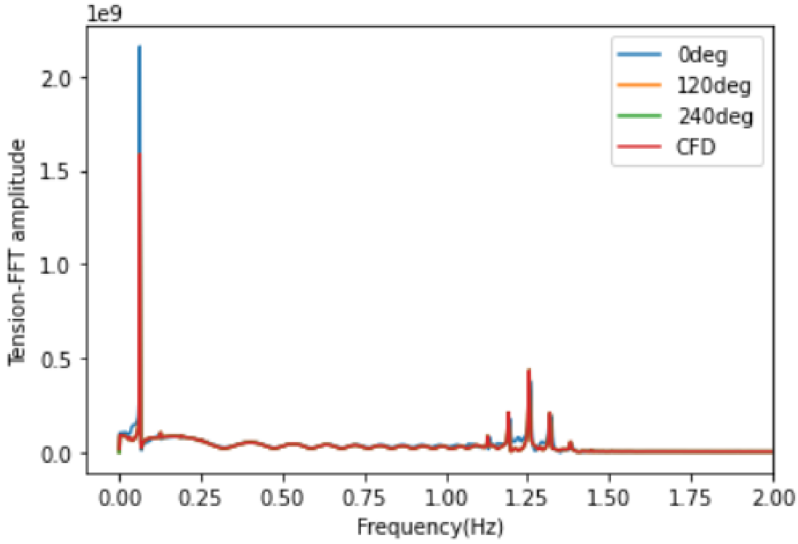

(b)

Fig. 4.16 The tendon tension response compared result and frequency domains.

Figure 4.16 shows the tension time history curve and energy spectrum results of TLP under extreme sea conditions. In the energy spectrum of the tension, the wave frequency response dominates, and the pitch and heave resonance response components of the platform can be seen. In the early stage of the simulation calculation, the tension on the tendon experienced high-frequency vibrations. The CFD calculation result can reach a maximum tension of 3.5MN, but the potential flow theory calculation result is not so large and the time required for high frequency attenuation, the potential flow theory takes longer than simulated by CFD, which is what we expected. Finally, the simulation calculation reached a steady state, and the tension on the tendon calculated by the two methods showed a good consistency, which is about 1MN to 2.2MN.

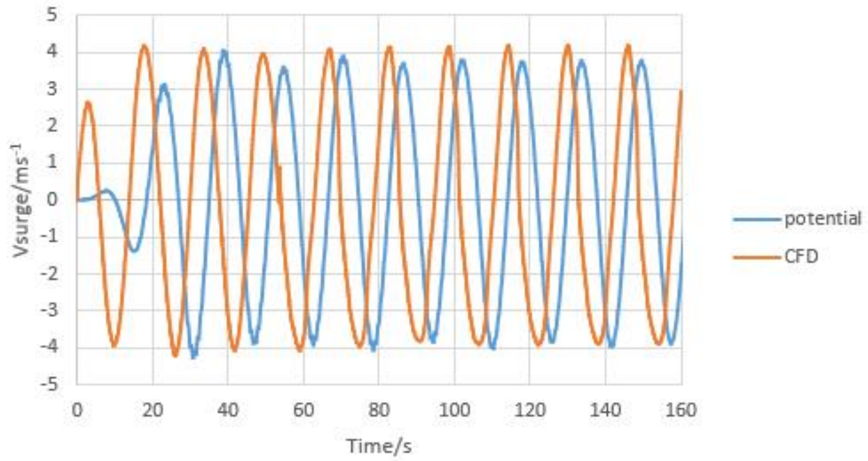

Fig. 4.17 TLP velocity in surge way compared result

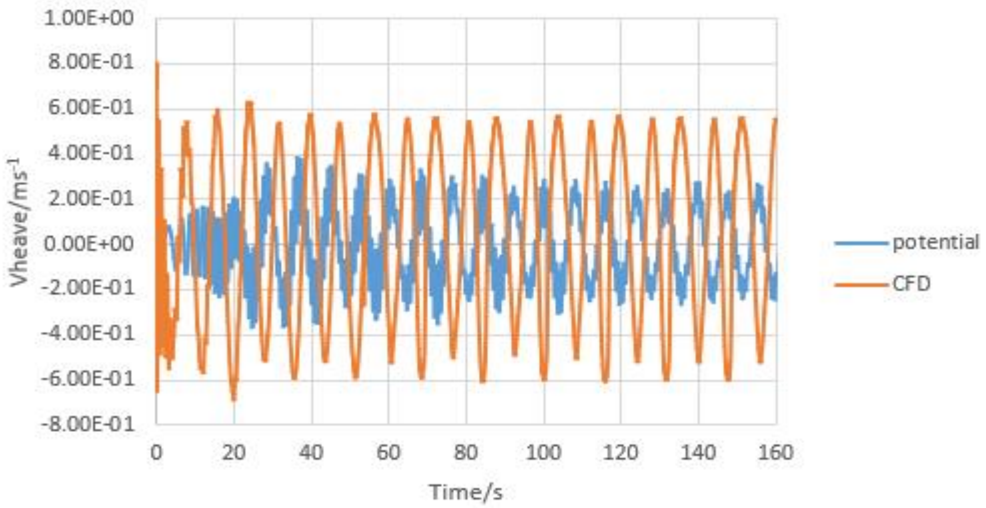

Fig. 4.18 TLP velocity in heave way compared result

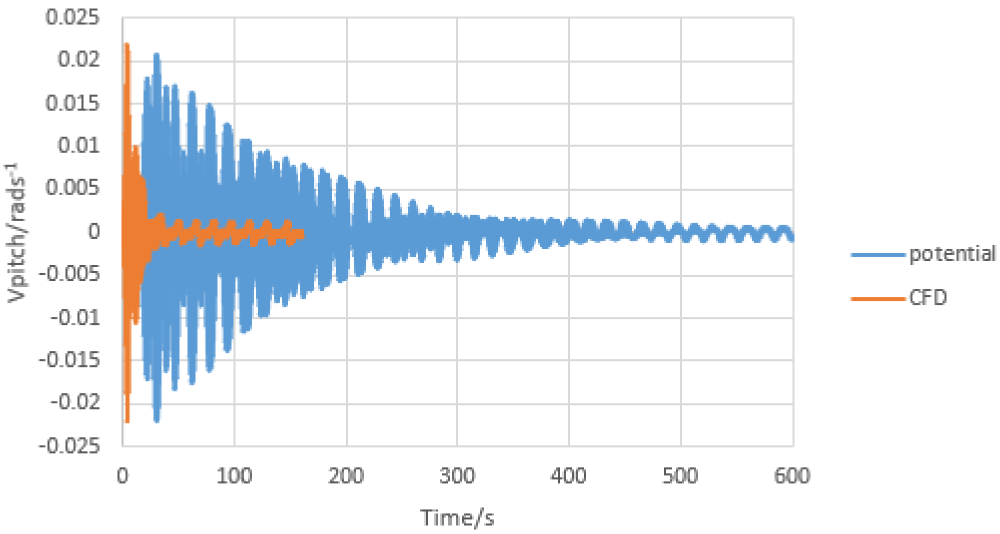

Fig. 4.19 TLP velocity in pitch way compared result

The three graphs shown above reflect the comparison of velocity changes in the three directions of surge, heave, and pitch calculated by CFD and potential flow theory, which can indirectly reflect the wave force and bending moment on TLP. It can be seen from the figures that the CFD calculation results of the total wave force in the wave transmission direction and the gravity direction are greater than the potential flow theoretical calculation results, while the y-axis bending moment CFD calculation results are smaller than the potential flow theoretical calculation results in the early stage of potential flow theory simulation calculation. As the calculation time increases, the results also tend to be consistent. This may be because compared with the simulation of potential flow theory, CFD calculation can better capture nonlinear effects, and can clearly reflect the influence of higher-order components in waves on the motion performance of the platform.

5. Conclusion

CFD simulations by OpenFOAM have been carried out to study the motion characteristics of a TLP. First, the CFD simulation on a well documented benchmark case, the floating block in regular waves was carried out, and it is found that present result agrees well to those in the literature, which verify the accuracy and reliability of the interFoam solver on solving the motion of such platforms in waves. On this basis, the motion response of each degree of freedom of the platform under extreme sea conditions, the time-history characteristics and energy spectrum characteristics of the platform bending moment and the force of the mooring system are investigated. The CFD results are also compared with the results obtained by a potential flow theory. The main conclusions are as follow:

The main components of the TLP motion in waves, the y-direction bending moment of the platform and the tension of the mooring system, are studied in this research, on both the wave frequency response and the resonance response. Regarding TLP pitch, more nonlinear response components can be seen compared with surge and heave. This is due to the nonlinear wave force on the platform and the time-dependent variation of the wet surface of the platform. In extreme sea conditions, the surge motion of the platform is less affected by the high-order components of waves, while the pitch motion is more easily affected by the high-order components.

The CFD simulation results are more sophisticated than the potential flow theory results, which can capture the high-order components of the wave and display the detailed flow field image. The nonlinearity of the radiation and diffraction phenomena of waves by the existence of the structures, is stronger under extreme sea conditions.

The agreement between CFD model and potential flow theory model is good, which provides confidence for the further application of the proposed CFD model.

In the present study, the authors demonstrate relatively good agreement between CFD results and results based on potential flow theory at a wave height of ten meters. For future work, the focus will be on the possibility of shifting to larger wave heights, such as twenty meters wave heights, for more extreme sea conditions. A CFD model will be used to study TLP in irregular waves under extreme ocean conditions. In this case, non-linear effects such as wave breaking, deck surf, etc. are likely to occur. The nonlinear wave-induced response determined by the CFD method will be analyzed and compared with the results of the potential flow theory.

References

[1] 国内外の浮体式洋上風力発電プロジェクト事例

[2] TLP 方式による浮体式洋上風力発電 低コスト化技術検証事業の採択について, URL: https://www.jera.co.jp/information/20220121_827

[3] 3D-numerical analysis of wave-floating structure interaction with OpenFOAM, Agnese Paci, Maria Gabriella Gaeta, Alessandro Antonini, Renata Archetti DICAM, University of Bologna

[4] Numerical study of the dynamic response of a wind turbine on a tension leg platform with a coupled partitioned six degree-of-freedom rigid body motion solver, Jeng Hei Chowa, Eddie Y.K. Nga, Narasimalu Srikanth, Ocean Engineering 172(2019)575-582

[5] Study of real floating structures under severe weather conditions, Barajas, G., Lara, J.L., Di Paolo B., Maza M., Losada, Í. J., Coastal Hydrodynamics and Infrastructure Group "The Environmental Hydraulics Institute IHCantabria

[6] Comparison of wave load effects on a TLP wind turbine by using computatioanal fluid dynamics and potential flow theory approaches, Ali Nematbakhsh, Erin E. Bachynski, Zhen Gao, Torgeir Moan, Applied Ocean Research 53 (2015) 142-154

[7] Stability Analysis of a TLP with Inclined Tension Legs under Different Marine Survival Conditions, Naying Wei, Zhen Zhang, Xu Xu, Wenjuan Yao, Journal of Marine Science and Engineering, 31 July 2022

[8] OpenFOAM predictions of hydrodynamics loads on full-scale TLP, Shaoshi Dai, Bassam A. Younis, Liping Sun, Ocean Engineering 102 (2015) 162-173

[9] ナビエ・ストークス方程式, 春日 悠, 2016.2.2.3

[10] InterFoam, URL: https://openfoamwiki.net/index.php/InterFoam

[11] OpenFOAM: User Guide v2112 k-epsilon, URL: https://www.openfoam.com/documentation/guides/latest/doc/guide-turbulence-ras-k-epsilon.html

[12] Dynamic meshes in OpenFOAM, Online Training – Advanced session July 2021, wolf dynamics

[13] User Guide: Stokes II – OpenFOAM, URL: https://www.openfoam.com/documentation/guides/latest/doc/guide-wave-regular-stokesii.html

[14] CFD numerical analysis of hydrodynamic and kinematic performance of a STLP, AN Xiaoting, ZHAO Weiwen, WAN Decheng, THE OCEAN ENGINEERING Vol. 38 No. 5 Sep. 2020

[15] Offshore wind power Energy For Maine, URL: https://newenglandaquaventus.com

[16] Floating Offshore Wind Foundations, URL: https://www.esubsea.com/floating-offshore-wind-foundations/

[17] OpenFOAM Lecture Course Series 2010-5,6 blockMes と snappyHexMesh を用いた格子生成, OpenFOAM 非圧縮性流体解析演習シリーズ, 今野 雅（オープン CAE 学会、東京大学）

[18] Experimental Validation of the Computation Method for Strongly Nonlinear Wave-Body Interactions, Changhong HU, Masashi KASHIWAGI, Research Institute for Applied Mechanics, Kyushu University

[19] Numerical and experimental study on a 2-D floating body under extreme wave, Xizeng Zhao, Changhong Hu, Applied Ocean Research, Applied Ocean Research 35 (2012) 1–13

[20] Python Numerical Methods, FFT in Python, URL: https://pythonnumericalmethods.berkeley.edu/notebooks/chapter24.04-FFT-in-Python.html

Acknowledgements

First of all, I am very grateful to Professor Changhong Hu for accepting me as a member of his lab and taking care of me during this period of time. Professor Hu gave me the opportunity to study at Kyushu University and I cherish this opportunity very much.

I would also like to thank Prof. Mohamed M. Kamra and Prof. Seiya Watanabe for their help in my study and patiently answering my questions. Thanks to Secretary Yoshizu for his enthusiasm and support.

I would also want to say thanks to my enthusiastic classmates and seniors. Baba Shohei, Noma Yuuki, etc., and the other first and second year students, I really had a great time with them.

Most importantly, I would like to thank my parents and grandma, they make me live a happy life, they have continuously supported me and encouraged me, they will always be my strongest supporters.

Even though it is only a short year at Kyushu University, I will never forget this precious memory.

The computation was carried out using the computer resource offered under the category of General Projects by Research Institute for Information Technology, Kyushu University.